Synthesis, Characterization of Novel *N*′(2-Phenoxyacetyl)Nicotinohydrazide and *N*′(2-Phenoxyacetyl)Isonicotinohydrazide Derivatives as Anti-Inflammatory and Analgesic Agents

H. M. Pallavi
University of Mysore
Fares Hezam Al-Ostoot
University of Mysore
Hamse Kameshwar Vivek
Adichunchanagiri Institute of Medical Sciences
Shaukath Ara Khanum (shaukathara@yahoo.co.in)
University of Mysore https://orcid.org/0000-0003-4571-6419

Research Article

Keywords: Synthesis, Nicotinohydrazide, Anti-inflammatory, Analgesic, Molecular modeling.

Posted Date: July 7th, 2021

DOI: https://doi.org/10.21203/rs.3.rs-657492/v1

Abstract

A new derivatives of isonicotinohydrazide **9 (a-e)** and **10(a-e)** were designed, synthesized, characterized based on the different spectroscopic analysis FT-IR, -^{1}H, -^{13}C-NMR, mass spectra, and also elemental-analyses, and identified as a remarkable anti-inflammatory along with analgesic effect. *In-vitro* and *in-vivo* anti-inflammatory and analgesic actions were performed using analgesic acetic acid-induced squirming and Hot plate latency tests using male Swiss albino mice. The study was supported by the in-*silico* and ADMET approaches. Among the series, compound (**10e)** showed the highest IC_{50} value for COX-1 inhibition, whereas compounds (**9e)** and (**10e)** exhibited the highest COX-2 SI. Further, *in silico* studies provide a putative bind site for the potent compound in a three-dimensional geometrical view. The results revealed that the title compound (**10e)** with bromo group exhibited potent COX-2 inhibitor at different times which is on par with the normal drug used in the assay system. Substitution of halogens at *N*′(2-phenoxyacetyl)nicotinohyrazide showed (**10e**) potent analgesic outcome on acetic acid-induced squirming response and thermal pain among the series **9(a-e)** and **10(a-e)**. The overall pharmacological result suggests that the newly synthesized compounds possess good anti-inflammatory along with analgesic-activity which was evaluated through *in-vitro, in-vivo*, and –*silico* studies.

1. Introduction

Inflammation is a complex multifactorial immunological cascade operated by several factors [1]. Primarily during tissue damage, PLA_2 is the first enzyme that provides the substrate for cyclooxygenase (COX) [2]. The two important cyclooxygenases COX-1 and COX-2 are two important enzymes to keep the homeostasis in health and injury, which is very vital [3]. The substrate for COX is obtained from the catalysis of phospholipid by secretory prostaglandins ($sPLA_2$). Thus, the product of $sPLA_2$ which is arachidonic acid (AA) is converted to pro-inflammatory and inflammatory PG by COX-2, which is the main causative for driving inflammatory cascade. Whereas in the case of COX-1, the AA metabolites are very important in keeping homeostasis of vascular tone and blood clotting cascade for the normal physiological conditions [4]. Hence, the activity of $sPLA_2$ is directly proportional to COX's enzyme catalysis. Diclofenac and Indomethacin are nonsteroidal anti-inflammatory drugs (NSAIDs) which are used worldwide for considering inflammatory disorder such as osteoarthritis, asthma, cancer, inflammatory intestine ailment, rheumatic arthritis, allergy, and atherosclerosis [5, 6]. NSAIDs block the COX-2 inducible isoform which prevent the biosynthesis of prostaglandins. In other hand COX-1 is housekeeping enzyme which is helps in homeostatic functions, which includes vascular antithrombotic activity, cytoprotection of such as gastric mucosal [7]. The development of specific COX-2 inhibitors with non-reactive COX-1 along with fewer or no side effects has been the main attractive target for many researchers for many decades [8–10]. Heterocyclic compounds have a versatile role in the area of different fields of sciences such as chemistry, biology, biochemistry, drug design, and medicinal chemistry [11]. Heterocycles containing nitrogen are known to possess various pharmaceuticals applications [12, 13]. This has attracted many researchers attention in recent year and it is one of the most important division which have an amazing activities in pharmacy [14], agriculture [15], the polymer [16] and other fields [17]. The main biological activities of nitrogen-containing compounds are antiproliferative [18], antiviral [19], antimalarial [20], anti-inflammatory [1] and antimicrobial [21]. Further, the literature reveals that pyridine is the most prevalent heterocyclic compound in nature. It plays a versatile part as a building block in the synthesis of biologically active compounds in nature. Pyridine and its derivatives are significant chemical with remarkable relevance in diverse fields [22]. Besides, Pyridine derivatives account for various biological activities and a great number of the derivatives are used in many recent clinical trials. Substituents on the pyridine nucleus enhance the approach towards the various biological targets which could fit into the active site of enzymes, proteins and DNA [23].

Moreover, the chemistry of hydrazide derivatives has been obtained great concern in both areas of organic chemistry and as well as biological science with striking impact [24]. The proton in hydrazides has been considered as a classic compound for the new drug invention [25]. Therefore, researchers have been shown a great concern in developing these derivatives as target structures for significant evaluation of the new biological activities [26]. Furthermore, compounds bearing phenoxy moiety are also involved in anti-inflammatory activity [27]. Interestingly nitrogen-containing heterocycles, in particular pyridine, have been commonly found as a structural unit in synthetic anti-inflammatory and analgesic drugs such as etoricoxib, epibatidine, piroxicam, niflumic acid, ABT-594 (5-(2-azetidinylmethoxy)-2-chloropyridine), and flunixin [28–32] as shown in Fig. 1. The aim of the presnt study was to determine the effectiveness of newly synthesized compounds as anti-inflammatory and analgesic compounds. In this context and based on our previous work [1, 2, 4, 7, and 27], the present research work emphasizes amalgamation and anti-inflammatory action of nictinohydrazide **9**(**a-e**) and isonictinohydrazide derivatives **10**(**a-e**).

2. Result And Discussion

2.1. Structure-based design

To begin with, a sufficient investigation in the literature survey was done to make known the importance of the nitrogen-containing heterocyclic compounds, for instance, pyridine analogs [23] and phenoxy acetyl analogs were found to have potent anti-inflammatory activities. Besides, drugs etoricoxib, epibatidine, piroxicam, niflumic acid, ABT-594 and flunixin, consist of a pyridine ring and are prominent anti-inflammatory inhibitors. But, the newly synthesized compounds contain the necessary pharmacophore which helps the prominent binding position of COX-2. The major prerequisite for an inhibitor to bind at the active position of COX-2 is its lipophilicity nature as the enzyme cleaves a lipophilic substrate so it is a major requirement for an inhibitor to be hydrophobic. Hence the substitutions were carried out on the pyridine ring as a lipophilic ring, along with the nitrogen atom for establishing hydrogen bonding the existence of a distal phenoxy ring. Amide oxygen establishes a hydrogen bond with Arginine amino acid present at the active position of COX-2. Based on these criteria we have designed and synthesized novel analogs **9(a-e)** and **10(a-e)** which have amide oxygen, lipophilicity, and other necessary pharmacophores (Fig. 2).

2.2. Chemistry

The processes to the synthesis of the target analogs **9(a-e)** and **10(a-e)** is demonstrated in Scheme1. The title compounds were identified by spectral data of IR, NMR, and mass spectroscopy. Compound (**3a)** spectrum served as an example to represent the structures of the amide **3(a-e)** series. The formation of target compound (**3a)** was established by witnessing the vanishing of the OH stretching band of compound (**1**) and the presence of a new ester carbonyl

group stretching band at 1730 cm^{-1} in the IR absorption range. However, the NMR spectrum exposed the vanishing of wide-ranging singlet for the hydroxy group of compound (**1**) and the presence of a triplet for CH_3 and quartet for CH_2 protons at δ 1.20 and 4.22 ppm of compound (**3**) respectively. Also, the mass spectrum contributed noteworthy stable M + at *m/z* 180, which established the creation of compound (**3a**). In addition, (**4a**) compound spectrum served as a model to elucidate the spectral data for the **4(a-e**) compounds. This was verified by vanishing the carbonyl group extending band in the IR absorption band for the ester group of compound (**3a**) and the advent of carbonyl and OH stretching bands of the COOH group of compound (**4a**) at 1730 and 3430–3510 cm^{-1}. Similarly in NMR data, there is a vanishing of the triplet for CH_3 and quartet for CH_2 protons of compound (**3a**) and the advent of COOH proton at δ 13.05 ppm, whereas the mass spectrum contributed noteworthy steady M + at *m/z* 152. Similarly, the bands of compounds (**6** and **8**) established by the exhibition of NH and NH_2 extending bands in the series of 3120–3224 and 3130–3230 cm^{-1} respectively, and carbonyl group bands at 1669 and 1669 cm^{-1} respectively, in the IR band. Remarkably, in the proton NMR, the presence of two singlet peaks for NH_2 and NH protons between δ 4.43 and δ 9.62 ppm respectively, established the creation of compounds (**6** and **8**). Also, the mass spectrum of compounds (**6** and **8**) showed a significant M + peak at *m/z* 137 and 137 respectively. Lastly, compound (**9a)** is well-thought-out as an illustrative example for the **9(a-e)** and **10(a-e)** series. In the IR spectrum of the compound (**9a**), the NH_2 absorption band of compound (**6**) and the carbonyl and OH stretching band of compound (**4a)** vanished. Whereas new stretching bands at 1648 cm^{-1} for amide carbonyl and in the range 3131–3237 cm^{-1} for the NH-NH group were present. In the NMR spectrum, the COOH proton peak of compound (**4a)** vanished and a new peak for amide proton at δ 10.30 and 10.62 ppm showed up. Lastly, the mass band of compound (**9a)** showed an M + peak at *m/z* 272 which confirmed the establishment of the main compound (**9a**) as shown in Supplementary Fig. 1–3.

2.3. Biology:

2.3.1. *In-vitro* COX inhibition

The newly title compounds **9(a-e)** and **10(a-e)** were screened to evaluate their efficacy to inhibit human COX-1/COX-2 by an *in-vitro* assay system. The competence of title compounds **9(a-e)** and **10(a-e)** was found by assessing their peroxidase action. Wherein, the standard drugs such as celecoxib, diclofenac, and indomethacin were used during the assay. Four-parameter logistic (4PL) dose-dependent activity curves (Fig. 3a and 3b) for each compounds **9(a-e)** and **10(a-e)** were calculated and tabulated in Table 1. The inhibitory action of title compounds and standard compounds were represented as IC_{50} values. The Selectivity Index (SI) was evaluated [IC_{50} (COX-1)/IC_{50} (COX-2)] as presented in Table 1. The *in-vitro* assay exposed that the novel title compounds **9(a-e)** and **10(a-e)** efficiently inhibit COX-1/COX-2 with varied groups in their nucleus. The compounds **9(a-e)** and **10(a-e)** exhibit loose binding efficiency with an IC_{50} value ranging from 6.907–11.107 μM as a compared standard inhibitor and their selective indexes for COX-1 inhibitor (indomethacin, IC_{50} = 0.041 μM) and the nonselective COX-1 inhibitor (diclofenac, IC_{50} = 4.802μM). In addition, the newly title compounds **9(a-e)** and **10(a-e)** inhibit sufficient COX-2 inhibition (IC_{50} = 0.095–0.263 μM) compared to the selective COX-2 inhibitor (celecoxib, IC_{50} = 0.091 μM) and diclofenac(IC_{50} = 0.822μM). Also, COX-1 and COX-2 data is represented graphically as shown in **Figs. (4a)** and **(4b)**.

Among the series **9(a-e)** and **10(a-e)**, compounds (**9b**, **9c**, **9e**, **10a**, **10b**, **10c** and **10e)** showed active COX-2 inhibition (IC_{50} = 0.095–0.165 μM) and the IC_{50} values are close to standard drug celecoxib. Whereas the remaining compounds (**9a**, **9d**, and **10d)** showed the least effectiveness in the direction of COX-2 inhibition (IC_{50} = 0.207 to 0.263 μM). Concerning a COX-2 SI, compounds (**9e)** with electron-withdrawing bulky bromo group at the para location in nicotinic hydrazide ring and (**10e)** with bromo group at the para location in isonicotinic hydrazide ring showed the maximum SI values (SI = 99.11 and 116.91 respectively). However (**9b, 9c, 10a, 10b** and **10c)** compounds displayed reasonable COX-2 SI values (SI = 54.64–99.04). On the contrary, compounds (**9a)** with no substituent, (**9d** and **10d)** with an electron-donating methyl group, exhibited lesser SI values (SI = 38.29, 33.36 and 32.66 respectively) as shown in Table 1.

2.3.2. *In-vivo* anti-inflammatory activity of compounds 9(a-e) and 10(a-e)

In-vivo anti-inflammatory activity for compounds **9(a-e)** and **10(a-e)** were estimated along with a normal drug-using formalin-induced rat paw edema model. Subcutaneous formalin was injected into the rat paw to induce severe inflammation. Edema so induced was treated with the **9(a-e)** and **10(a-e)** compounds along with standard drug (10 mg/kg b.wt) to assess the percentage of edema inhibition was observed after a time duration of 1, 2, 3, and 6 hr respectively (Fig. 5a-d). The outcome showed an extensive range of anti-inflammatory activity (12.93–51.99 %; 1 hr), (19.45–57.21 %; 2 hr), (14.98–64.92 %; 3 hr) and (10.01–45.95 %; 6 hr) in accordance with the normal compound diclofenac (30.32 %;1 hr, 25.42 %; 2 hr, 22.86 %; 3 hr, 22.88 %; 6 hr) as shown in Table 2. Among the series **9(a-e)** and **10(a-e)**, compounds (**9c)** with dual chloro groups at ortho and para location, (**10a)** without any substituent, **(10b)** with chloro group at the para location, and **(10e)** with bromo group at the para location, in phenoxy ring showed additional anti-inflammatory activity after 1hr. Interestingly the compounds (**10e)** (51.99 %edema inhibition) with electron-withdrawing bromo-group at the para location and (**10b)** (51.76 % edema inhibition) with the chloro-group at para position possessed potent activity compared to diclofenac (30.32 % edema-inhibition). Further, the compounds (**9d**) (25.75 % edema-inhibition) and (**10d)** (12.93 % edema inhibition) with electron releasing methyl group exhibited lower potency. While after 2 hr, compound (**10e**) (57.21 % edema inhibition) displayed the highest anti-inflammatory activity, and compounds (**9c**) (55.71 % edema inhibition) and **(10b)** (55.75 % edema inhibition) showed the next highest activity. Surprisingly even after 2 hr compounds (**9d)** (20.51 % edema-inhibition) and (**10d)** (19.45 % edema inhibition) exhibited lower potency as related to the normal (diclofenac 25.42 % edema inhibition). Once again after 3 hr also compound (**10e)** (64.92 % edema-inhibition) displayed the highest anti-inflammatory activity and compounds (**9c)** (60.89 % edema inhibition) and **(10b)** (60.91 % edema inhibition) exhibited the next highest activity. Besides, the compound (**9d)** (14.98 % edema inhibition) showed the least activity as related to the normal diclofenac with 22.86 % edema inhibition. Finally, after 6 hr also the same compound (**10e)** (45. 95 % edema inhibition) along with compounds (**9e)** (45. 85 % edema inhibition) and **(10b)** (45. 82 % edema inhibition) shown the highest anti-inflammatory action related to the normal diclofenac with 22.88 % edema inhibition. Collectively, compound (**10e)** with IC_{50} value 7.75 μM, exhibited encouraging anti-inflammatory activity at 1, 2,-3, and 6-h time interludes and had additional effect than diclofenac (IC_{50} value 9.7 μM). To conclude the *in-vivo* efficacy, the anti-inflammatory action of title compounds **9(a-e)** and **10(a-e)** inveterate that phenoxy ring bearing acetyl and nicotinohydrazide moiety accomplished active anti-inflammatory activity (Fig. 6).

The potent compound is interacting with COX mediated inflammatory pathway wherein arachidonate metabolism that produces prostaglandins is arrest the release of inflammatory mediators [33].

2.3.3. Analgesic activity of the title 9(a-e) and 10(a-e) series

Analgesic activity for the newly title compounds **9(a-e)** and **10(a-e)** were evaluated by the acetic acid-induced writhing test and the hot plate latency test.

2.3.3.1. Acetic acid-induced writhing test.

The intraperitoneal administration of acetic acid will induce essential nociception and peripheral actions [34]. The outcome of the acetic acid-induced writhing test for, the title compounds **9(a-e)** and **10(a-e)** suggest that the analgesic activity of the compound (**10e)** showed 63.48 % inhibition, which is close to the standard piroxicam (63.99 % inhibition). In the case of compound (**9b)** (57.55 % inhibition) and (**10c)** (62.67 % inhibition) exhibited good activity which is tabulated in Table 3. While compounds (**10a)** (53.94 % inhibition) and (**10b)** (47.66 % inhibition) exhibited moderate analgesic activity. Conversely, it was noted that there was a considerable decrease in mice receiving the compounds (**9a, 9c, 9d, 9e**, and **10d)**, and the efficacy in inhibiting the writhing response was between 23.34–38.89 %. Concerning the SAR, it was seen that the action of large halo mixtures (**9b**) (IC_{50} value 7.9 μM), (**10c**) (IC_{50} value 5.9 μM), and **(10e)** (IC_{50} value 5.9 μM) with the chloro group at para location, two chloro groups at ortho and para location and bromo group at the para location in the phenoxy ring were found to be more powerful than compounds (**9d)** (IC_{50} value 11.9 μM) and **(10d)** (IC_{50} value 10.7 μM) with an electron-donating methyl group at the para position in the phenoxy ring (Fig. 7).

2.3.3.2. Hot plate latency test

The pain-induced hot plate precisely affects centrally mediated nociception. To test the newly title **9(a-e)** and **10(a-e)** possess central analgesic activity, this was performed as per the guidelines and evaluation narrator by Williamson et al., [35]. The external administration of the main compounds **9(a-e)** and **10(a-e)** prolong the latency time as compared to basal values. In this assay, compounds (**10c)** (84.91 %) and **(10e)** (89.95 %) exhibited increased pain level after 1hr. Notably, there was a surge in pain after 2 hr, and the values obtained were the same in the case of compounds (**10c)** (49.29 %) and **(10e)** (56.64 %). this shows a lessening in nociception by the compounds (Table 4). Overall, series **9(a-e)** and **10(a-e)**, compounds (**10c)** with two chloro groups at ortho and para position and (**10e)** with the bromo group at the para position in the phenoxy ring showed a potent central analgesic activity at 1hr which is similar to the piroxicam normal drug (76.70 %). Attractively, compounds such as (**9d** and **10d**) with a methyl group at the para position in the phenoxy ring showed decrease potency after 1 hr (26.95 and 12.23 % respectively) and were followed by subsequently hours. Besides, compounds (**9a, 9b, 9c, 9e, 10a**, and **10b)** showed moderate analgesic activity in the range 41.73–49.97 % at 1 hr and 35.99–45.93 % at 2 hr. The accomplished results obtained were comparable with the *in-vitro* COXs result. The result obtained by the hot plate latency test reveals that the newly title compounds **9 (a-e)** and **10 (a-e)** possess analgesic activity along with anti-inflammatory potency.

2.4. Molecular docking and ADME/Tox

Molecular docking studies play an important role to identify the probable binding orientation of each molecule inside the active site pocket *in-silico* [39]. Thus, we analyzed the binding pose of the potent inhibitor with the crystal structure of the downstream inflammatory enzyme such as COX. The primary enzyme which initiates the activity of the COX-2 is $sPLA_2$ [37]. Inflammation is a complex immunological pathway, characterized by tissue damage and up-regulation of $sPLA_2$. The product of $sPLA_2$ which is arachidonic acid is the substrate of two main enzymes, cyclooxygenases (COX) and lipoxygenases (LOX), which are recognized for their important role in generating numerous prominent biological mediators [33]. The inhibition of COX-2 eventually down-regulates the synthesis of pro-inflammatory prostaglandins (PGs) and leukotrienes (LTs), which is widely studies and remains the main focus of many researchers to target the COX-2 to inhibit the inflammatory pathway. COX-1 isozyme plays an important role in maintaining a normal physiologic state of vital organs such as gastrointestinal (GI) mucosa, platelets, endothelium, kidneys, uterus, and also act as cytoprotective activity [38]. In the present study, molecular docking studies revealed that ligand (**9e** and **10e)** docked into the active site of COX-2 very efficiently. Ligand (**9e)** forms *π-π* stacking with Trp387 (Supplementary Fig. 4), ligand (**10e)** forms *π-π* stacking with Trp387 and Typ385 (Fig. 8) with COX-1. The ligand (**9e)** forms *π-π* stacking with Typ385 and hydrogen bond with Ser530 (Supplementary Fig. 5) whereas ligand (**10e)** forms *π-π* stacking with Typ385, Tyr355 and Trp387 and hydrogen bond with Arg120 (Fig. 9) with the docking score and hydrogen bond of -8.98 and − 0.35 kcal/mol respectively (Table 5) which is more efficient binding with the active site receptor. These amino acid residues exhibits a significant part in the catalysis of COX-2 [39], thus, the interaction with these amino acid residues will probably down-regulate the activity of COX-2. *In-silico* ADME/Tox computation of the synthesized compounds gives a brief knowledge about absorption, distribution, metabolism, and excretion also toxicological evaluation. Based on an *in-silico* study of our newly synthesized compounds revealed that the compounds safely pass through ADME/Tox studies, this is based on the cut-off values which come across within the standard range (Table 6) possessed by nearly 95 % of available drugs.

3. Conclusion

To conclude, a series of *N*(2-phenoxyacetyl) nicotinohydrazide **9**(**a-e**) and *N*(2-phenoxyacetyl)isonicotinohydrazide derivatives **10**(**a-e**) were skillfully designed and synthesized by substituting functional groups such as bromo, chloro, and methyl groups at various positions at the phenoxy ring to induce potent analgesic and anti-inflammatory activity. The results revealed that the title compounds **9(a-e)** and **10(a-e)** exhibited potent COX-2 inhibitor which is similar to the typical drug used in the assay system. Furthermore, the compound (**10e)** with bromo group exhibited good anti-inflammatory activity at different time intervals such as 1, 2, 3, and 6 hr, and was more effective than diclofenac. Substitution of halogens at *N*′(2-phenoxyacetyl)nicotinohyrazide showed (**10e**) potent analgesic effect on acetic acid and produced writhing response and thermal pain among the series **9(a-e)** and **10(a-e)**. The overall pharmacological result suggests that the title synthesized compounds possess good anti-inflammatory along with analgesic activity which was evaluated *in-vitro, in-vivo*, and

in-silico studies. The molecular docking studies reveal the three-D interpretation of the potent ligand binding towards the assumed active location of COX-2 with different types of interactions.

4. Materials And Methods

All solvents, beginning material, and reagents were secured from “Sigma Aldrich Chemicals Private Limited” with purity 90–99 %. Systematic “Thin-Layer Chromatography” (TLC) was carried out on 0.25 mm silica gel plates (Merck 60 F 254) by utilizing a distinctive dissolvable framework that was pictured by UV light. The melting point was taken on a Chemi Line Micro Controller-based melting point device with an advanced thermometer. IR spectra were documented by the potassium bromide pellet strategy on Cary 630 FTIR Agilent spectrophotometer, NMR range was documented on a VNMRS-400MHz Agilent-NMR spectrophotometer in dimethyl sulfoxide (DMSO-d_6). The mass range was acquired with a VG70-70H spectrometer. Basic analysis results are within 0.4 % of the theoretically calculated rate.

4.1 Chemistry

4.1.1 Chemistry: Plan of the synthesis

The synthesis series of the title compounds *N*′(2-phenoxyacetyl)nicotinohydrazide **9**(**a-e**) and *N*′(2-phenoxyacetyl)isonicotinohydrazide derivatives **10**(**a-e**) were achieved by a synthetic process which is shown in Scheme 1. All the compounds produced were recognized by IR, NMR, and mass spectral data. At the start, a mixture of different phenols **1(a-e)** and ethyl chloroacetate (**2**) was refluxed with dry acetone which served as a solvent and produced the corresponding ester substituted ethyl-2-phenoxyacetates **3(a-e)**. The refluxing of compounds **3(a-e)** with sodium hydroxide solution along with ethanol provided substituted phenoxy acetic acids **4(a-e)**. Besides, ethyl nicotinate **(5)** was treated with 99 % hydrazine hydrate to furnish nicotinic hydrazide **(6)**. Similarly, ethyl isonicotinate **(7)** was treated with 99 % hydrazine hydrate to achieve isonicotinic hydrazide **(8)**. Finally, the intermediates compounds **4(a-e)** were treated with nicotinic hydrazide **(6)** along with lutidine, *O*-(benzotriazol-1-yl)-*N*, *N*, *N*, *N*-tetramethyluroniumtetrafluoroborate (TBTU), and dry dichloromethane (DCM) to afford *N*′(2-phenoxyacetyl)nicotinohydrazides **9(a-e)** in a good yield (63–72%). Correspondingly, *N*′(2-phenoxyacetyl)isonicotinohydrazides **10(a-e)** were synthesized in good yield (74–79%) starting from isonicotinic hydrazide **(8)**.

4.1.1.1 Common synthetic methods for ethyl-2-phenoxyacetate derivatives 3(a-e)

The substituted of phenols (**1a-e**, 0.06 mol), ethyl chloroacetate (**2**, 0.065 mol), and anhydrous potassium carbonate (0.065 mol) mixed in dry acetone (35 ml) were continuously refluxed for 10 hr. After cooling the mixture, the solvent was separated by distillation. To eliminate potassium carbonate the remaining mass was first triturated with ice water and then take out with ether (3 × 30 ml) which was first directly washed 10 % sodium hydroxide solution (3 × 30 ml) and then by distilled water (3 × 30 ml). It was then dried over anhydrous sodium sulfate and evaporated to get the corresponding series of ethyl-2-phenoxyacetates (**3a-e**).

4.1.1.2. Common synthetic process for phenoxy acetic acid derivatives 4(a-e)

The above ester compounds of (**3a-e**, 0.020 mol) were dissolved in the solvent of ethanol (15 ml) and a solution of sodium hydroxide (0.035 mol). Then water (5 ml) was added. After refluxing the mixture for 8 hr, the obtained mixture was first cooled and then treated with 3 N hydrochloric acids. The precipitate obtained was filtered and washed with cold distilled water. It was lastly recrystallized from ethanol to obtain the acid series of 4**(a-e)**.

4.1.1.3. Common synthetic process for nicotinohydrazide derivatives (6 and 8)

0.016 mol hydrazine hydrate was added to a solution of ethyl nicotinate (5, 0.016 mol) in ethanol (20 ml) and stirred for 4–6 h at room temperature. The solid separated was treated with water (50 ml), filtered, and then washed with distilled water (3 × 20 ml). Lastly, the solid obtained was dried under the vacuum and later recrystallized with ethanol to get nicotinohydrazide **(6)**. Similarly, isonicotinohydrazide **(8)** was produced from ethyl isonicotinate (**7**).

Nicotinohydrazide (6)

Yield 75 %; M.P. 155–157°C; FT-IR (KBr) vmax (cm^{-1}): 1669 (amide, C = O), 3120–3224 (NH-NH_2); ^{1}HNMR (400 MHz, DMSO-d6) δ (ppm): 4.43 (s, 2H, NH_2), 6.80–7.41 (m, 4H, Ar-H), 9.62 (s, 1H, NH); ^{13}C NMR (100 MHz, DMSO- d6) δ (ppm): 164.8, 148.7, 148.1, 135.3, 130.7, 125.1. LC-MS *m/z* 137 Anal. Calcd. for $C_6H_7N_3O$(138): C, 52.55; H, 5.15; N, 30.64. Found: C, 52.49; H, 5.10; N, 30.55 %.

Isonicotinohydrazide (8)

Yield 75 %; M.P. 155–157°C; FT-IR (KBr) vmax (cm^{-1}): 1,669 (amide, C = O), 3120–3224 (NH-NH_2); ^{1}HNMR (400 MHz, DMSO-d6) δ (ppm): 4.53 (s, 2H, NH_2), 6.80–7.41 (m, 4H, Ar-H), 9.62 (s, 1H, NH); ^{13}C NMR (100 MHz, DMSO-d6) δ (ppm): 167.2, 149.7, 149.7, 140.8, 121.7, 121.7. LC-MS *m/z* 137 [M+]. Anal. Calcd. for $C_6H_7N_3O$(138): C, 52.55; H, 5.15; N, 30.64. Found: C, 52.49; H, 5.10; N, 30.55 %.

4.1.1.4. Common synthetic process for *N*′(2-phenoxyacetyl)nicotinohydrazide 9(a-e) and *N*′(2-phenoxyacetyl)isonicotinohydrazide derivatives 10(a-e)

Substituted acids (**4a-d**) were added to the compound (**6**) in dry DCM (15 ml). Then lutidine (1.5 vol.), at temperature 25–30°C was added and stirred for 25 min at the same temperature. After cooling to 0–5 ^{0}C in an ice bath, TBTU (0.003 mol) was added slowly over 20 minutes maintaining the temperature below 5°C. Then the mixture was stored overnight and observed by TLC with hexane: ethyl acetate (3:1) system. After dilution with DCM (30 ml) the mixture was

washed with 10 % of sodium bicarbonate solution (3 × 30 ml). Lastly, the organic layer was washed with distilled water (3 × 30 ml), dried over anhydrous sodium sulfate, and concentrated to produce compounds **9(a-e)**. Similarly compounds **10(a-e)** were produced beginning from compounds (**8**) and (**4a-e**).

N' **(2-phenoxyacetyl)nicotinohydrazide (9a)**

Yield 63 %; M.P. 174–177°C; FT-IR (KBr) vmax (cm^{-1}): 1648 (amide, C = O), 3131–3237 (NH-NH); ^{1}HNMR (400 MHz, DMSO-d6) δ (ppm): 4.64 (s, 2H, OCH_2), 6.93-9.00 (m, 9H, Ar-H), 10.30 (s, 1H, NH), 10.62 (s, 1H, NH); ^{13}C NMR (100 MHz, DMSO-d6) δ (ppm): 167.5, 164.5, 158.1, 152.8, 148.8, 135.6, 129.8, 128.4, 124.0, 121.6, 115.1. LC-MS *m/z* 272 [M+]. Anal .Calcd. for $C_{14}H_{13}N_3O_3$(272): C, 61.99; H, 4.83; N, 15.49. Found: C, 61.58; H, 4.64; N, 15.20 %.

N' **(2-(4-chlorophenoxy)acetyl)nicotinohydrazide (9b)**

Yield 66%; M.P. 171–174°C; FT-IR (KBr) vmax (cm^{-1}): 1659 (amide, C = O), 3129–3231 (NH-NH); ^{1}HNMR (400 MHz, DMSO-d6) δ (ppm): 4.59 (s, 2H, OCH_2), 6.59–9.06 (m, 8H, Ar-H), 10.32 (s, 1H, NH), 10.52 (s, 1H, NH); ^{13}C NMR (100 MHz, DMSO- d6) δ (ppm): 166.3, 164.8, 156.2, 148.7, 148.1, 135.3, 130.9, 130.9, 130.7, 126.6, 125.1, 117.4, 117.4, 66.3. LC-MS *m/z* 305 [M+], 307 [M + 2]. Anal. Calcd. for $C_{14}H_{12}ClN_3O_3$(305): C, 55.00; H, 3.96; N, 13.75. Found: C, 54.98; H, 3.64; N, 13.20%.

N' **(2-(2,4-dichlorophenoxy)acetyl)nicotinohydrazide (9c)**

Yield 69 %; M.P. 176–179°C; FT-IR (KBr) vmax (cm^{-1}): 1646 (amide, C = O), 3129–3231 (NH-NH); ^{1}HNMR (400 MHz, DMSO-d6) δ (ppm): 4.48 (s, 2H, OCH_2), 6.69–9.06 (m, 7H, Ar-H), 10.08 (s, 1H, NH), 10.11 (s, 1H, NH); ^{13}C NMR (100 MHz, DMSO- d6) δ (ppm): 166.3, 164.8, 152.7, 148.7, 148.1, 135.3, 131.4, 130.7, 129.0, 128.0, 125.1, 121.5, 117.1, 65.8. LC-MS *m/z* 339 [M+], 341 [M + 2], 343 [M + 4]. Anal. Calcd. for $C_{14}H_{12}Cl_2N_3O_3$(339): C, 49.43; H, 3.26; N, 12.35. Found: C, 49.40; H, 3.20; N, 12.20 %.

N' **(2-(p-tolyloxy)acetyl)nicotinohydrazide (9d)**

Yield 72 %; M.P. 175–178°C; FT-IR (KBr) vmax (cm^{-1}): 1644 (amide, C = O), 3133–3241 (NH-NH); ^{1}HNMR (400 MHz, DMSO-d6) δ (ppm): 4.54 (s, 2H, OCH_2), 6.89-9.00 (m, 8H, Ar-H), 10.10 (s, 1H, NH), 10.21 (s, 1H, NH); ^{13}C NMR (100 MHz, DMSO- d6) δ (ppm): 166.3, 164.8, 155.1, 148.7, 148.1, 135.3, 130.7, 130.7, 130.0, 130.0, 125.1, 125.1, 114.2, 114.2, 66.3, 21.3. LC-MS *m/z* 286 [M + 1]. Anal. Calcd. for $C_{15}H_{15}N_3O_3$(285): C, 63.15; H, 5.30; N, 14.73. Found: C, 63.10; H, 5.20; N, 14.60 %.

N' **(2-(4-bromophenoxy)acetyl)nicotinohydrazide (9e)**

Yield 68 %; M.P. 176–179°C; FT-IR (KBr) vmax (cm^{-1}): 1648 (amide, C = O), 3143–3251 (NH-NH); ^{1}HNMR (400 MHz, DMSO-d6) δ (ppm): 4.52 (s, 2H, OCH_2), 6.98–9.02 (m, 8H, Ar-H), 10.13 (s, 1H, NH), 10.24 (s, 1H, NH); ^{13}C NMR (100 MHz, DMSO- d6) δ (ppm):

166.3, 164.8, 157.1, 148.7, 148.1, 135.3, 132.6, 130.7, 125.1, 118.3, 115.4, 66.3. LC-MS *m/z* 349 [M+], 351 [M + 2]. Anal. Calcd. for $C_{14}H_{12}BrN_2O_3$(349): C, 48.02; H, 3.45; N, 12.00. Found: C, 48.00; H, 3.34; N, 11.90 %.

N' **(2-phenoxyacetyl)isonicotinohydrazide (10a)**

Yield 74 %; M.P. 171–173°C; FT-IR (KBr) vmax (cm^{-1}): 1651 (amide, C = O), 3146–3251 (NH-NH); ^{1}HNMR (400 MHz, DMSO-d6) δ (ppm): 4.63 (s, 2H, OCH_2), 7.01–8.73(m, 9H, Ar-H), 10.73 (s, 1H, NH), 10.36 (s, 1H, NH); ^{13}C NMR (100 MHz, DMSO- d6) δ (ppm): 166.3, 164.8, 158.1, 149.7, 149.7, 140.8, 129.7, 129.7, 121.7, 121.7, 121.0, 114.3, 114.3, 66.3. LC-MS *m/z* 271 [M+]. Anal. Calcd. for $C_{14}H_{13}N_3O_3$(271): C, 61.99; H, 4.83; N, 15.49. Found: C, 61.88; H, 4.77; N, 15.45 %.

N' **(2-(4-chlorophenoxy)acetyl)isonicotinohydrazide (10b)**

Yield 76 %; M.P. 175–178°C; FT-IR(KBr) vmax (cm^{-1}): 1649(amide, C = O), 3145–3253 (NH-NH); ^{1}HNMR (400 MHz, DMSO-d6) δ (ppm): 4.66 (s, 2H, OCH_2), 7.00-8.74 (m, 8H, Ar-H), 10.34 (s, 1H, NH), 10.72 (s, 1H, NH); ^{13}C NMR (100 MHz, DMSO- d6) δ (ppm): 167.2, 164.4, 156.9, 150.8, 139.7, 129.6, 125.5, 121.7, 117.0, 66.7, 40.5. LC-MS *m/z* 306 [M+], 308 [M + 2]. Anal. Calcd. for $C_{14}H_{12}ClN_3O_3$(306): C, 55.00; H, 3.96; N, 13.75. Found: C, 54.98; H, 3.84; N, 13.60 %.

N' **(2-(2,4-dichlorophenoxy)acetyl)isonicotinohydrazide (10c)**

Yield 75 %; M.P. 177–180°C; FT-IR (KBr) vmax (cm^{-1}): 1653 (amide, C = O), 3147–3256 (NH-NH); ^{1}HNMR (400 MHz,DMSO-d6) δ (ppm): 4.65 (s, 2H, OCH_2), 7.03–8.83 (m,7H, Ar-H), 10.75 (s, 1H,NH), 10.42 (s, 1H,NH); ^{13}C NMR (100 MHz,DMSO-d6) δ (ppm): 166.3, 164.8, 152.7, 149.7, 149.7, 149.7, 140.8, 131.4, 129.0, 128.0, 121.7, 121.7, 121.5, 117.1, 65.8. LC-MS *m/z* 339[M+], 341 [M + 2]. 343 [M + 4]. Anal.Calcd. for $C_{14}H_{12}Cl_2N_3O_3$(339): C, 49.43; H, 3.26; N, 12.35. Found: C,49.40; H,3.20; N,12.30 %.

N' **(2-(p-tolyloxy)acetyl)isonicotinohydrazide (10d)**

Yield 77%; M.P. 182–185°C; FT-IR(KBr) vmax(cm^{-1}): 1651 (amide, C = O), 3144–3257 (NH-NH); ^{1}HNMR (400 MHz, DMSO-d6) δ(ppm): 4.61 (s, 2H,OCH_2),7.01–8.89 (m, 8H, Ar-H), 10.73 (s, 1H,NH), 10.43 (s, 1H,NH); ^{13}C NMR (100 MHz,DMSO- d6) δ (ppm): 166.3, 164.8, 155.1, 149.7, 149.7, 140.8, 130.7, 130.0, 130.0, 121.7, 114.2, 114.2, 66.3, 21.3. LC-MS *m/z* 286[M + 1], Anal.Calcd. for $C_{15}H_{15}N_3O_3$(285): C,63.15; H,5.30; N,14.73. Found:C,63.10; H,5.20; N,14.60 %.

N' **(2-(4-bromophenoxy)acetyl)isonicotinohydrazide (10e)**

Yield 79 %; M.P. 183–186°C; FT-IR(KBr) vmax (cm^{-1}): 1649(amide, C = O), 3138–3254(NH-NH); ^{1}HNMR (400 MHz, DMSO-d6) δ (ppm): 4.63 (s, 2H,OCH_2), 7.03–8.86 (m, 8H, Ar-H),10.63 (s, 1H,NH), 10.41 (s, 1H,NH); ^{13}C NMR (100 MHz,DMSO- d6) δ (ppm): 166.3, 164.8, 157.1, 149.7, 149.7, 140.8, 132.6, 132.6, 121.7, 121.7, 118.3, 118.3, 115.4, 66.3. LC-MS*m/z* 349 [M+], 351 [M + 2]. Anal. Calcd. for $C_{14}H_{12}BrN_3O_3$(349): C, 48.02; H,3.45; N,12.00. Found: C, 48.00; H, 3.30; N, 11.98 %.

4.2 Pharmacology

4.2.1 Biological assessment, animal models, and ethics

In-vivo anti-inflammatory and analgesic experiments were performed by using of male Swiss albino mice weighing between 20–25 g. Firstly, the mice were gestated in normal controlled conditions. The room temperature was maintained at 25 ± 1.5°C and the relative humidity at 55–90 %. The recommended standard feed with clean water was provided and the mice were kept for a week before starting the *in-vivo* experiments. Animal studies were performed under strict animal handle procedures according to the guidelines issued by the "Research Ethical Committee*"* of the Farooqia College of Pharmacy, Mysuru.

4.2.2. *in-vitro* COX inhibitory activity

COX-1 and COX-2 inhibitory analyses were performed for the newly title compounds **9(a-e)** and **10(a-e)** with the help of colorimetric enzyme immune assay [40]. Manufacturer protocol (Cayman Chemical) was followed to evaluate the inhibitory efficiency for newly produced compounds contrary to COX-1 and COX-2 which was found through a COX inhibitor screening assay kit [41]. Briefly, enzymes COX-1 and COX-2 were incubated in distinct containers along with a reaction mixture and for inhibitory studies, compounds were pre-incubated for 5 min with particular enzymes, the reaction was started by adding arachidonic acid (final concentration 1.1 mM) followed by TMPD and gestated for 5 min at temperature of 25°C. The production of oxidized *N, N, N*, *N*-tetramethyl-*p*-phenylenediamine (TMPD) at 590 nm measured the activity results, and the percentage inhibition was determined by using the below equation.

COX inhibiting activity (%) = $[(1- (A_1-A_2)] \times 100$

A_0

Where A_0 = is the absorbance of the control (without the test compound),

A_1 = is the absorbance in the presence of the test compound and

A_2 = is the absorbance sample blank (without TMPD).

Different concentrations of samples were used to calculate the values of IC_{50} by making use of the calibration curve.

4.2.3. Anti-inflammatory *in-vivo* activity

In-vivo anti-inflammatory activity for newly title compounds **9(a-e)** and **10(a-e)** was assessed by making use of a formalin-induced rat foot paw edema model [42]. The title compounds **9(a-e)** and **10(a-e)** (10 mg/kg, b.wt) were used to estimate anti-inflammatory efficiency along with the normal drug diclofenac at a concentration of 10 mg/kg body weight through oral route. Inflammation was induced by injecting a 6 % formalin solution subcutaneous to the plantar surface of the left hind paw. Percentage increase/decrease in edema was estimated by using a plethysmometer measured at different time intervals 1, 3, and 6 hr after injecting formalin and later compared with the right back paw of the animals as reference. The proportion of edema inhibition was represented as percentage paw-volume change in milliliters by comparing test and control values. The percentage inhibition of the inflammatory effect of the title compounds, compared to control, was calculated using the following expression.

% Inhibition = [Degree of inflammation by the (control group- test group)] × 100

Degree of inflammation by the control group

4.2.4. Analgesic activity

4.2.4.1. Acetic acid-induced writhing test.

The acetic acid-induced test was performed by methods [43, 44] mentioned earlier. In brief, newly title compounds **9(a-e)** and **10(a-e)** about 10 mg/kg of body weight of mice was used in the treated group, 0.75 % of physiological saline used as a vehicle, standard piroxicam was taken at the concentration of 10 mg/kg, body weight. Target compound and the standard drug were given *via* oral route before 30 min injecting 0.7 % acetic acid solution (10 ml/kg, b.wt) at intra-peritoneal. The mice were monitored. The count of writhing movements like abdominal contraction successes by extension and dorsiflexion were recorded. The outcomes are represented as the number of writhes per 30 min period from which the proportion inhibition of writhing was determined using the formula.

Inhibition % = Mean No. of writhes (Control) - Mean No. of writhes (Test) × 100

Mean number of writhes (control)

4.2.4.2. Hot plate latency test.

A hot plate latency test was performed using the protocol [45] described earlier. The animals received standard saline (Control) or trial agents (10 mg/kg; body weight) along with the standard drug piroxicam (Positive control) at 0, 1, and 2 hr after administration respectively. The newly title compounds **9(a-e)** and

10(a-e) were administered orally one hour before initiating the experiment. The mice were then placed on a hot plate and the temperature was set to 50°C. The difference in time gave the response latency. The increase in baseline (in percentage) was calculated by the formula.

[Reaction time ×100]-100

Baseline

4.2.5. Statistical analysis

One-way ANOVA with significant $p < 0.05$ was used to compare between different groups Graphed prism was used for all statistical data calculations.

4.3. Molecular docking

The crystal coordinates of both enzyme COX-1 and COX-2 were taken from the "*Brookhaven Protein Data Bank"*, with [PDB id 3KK6] and [4COX] [36, 37]. 2D sketcher was used to place ligands **9(a-e)** and **10(a-e)** in the workspace. The force field OPLS 2005 was applied for energy minimize. Proteins were made by repossessing into the workspace. By using the protein pep wizard, the structure of the protein like the missing loops was corrected.

Water molecules that were beyond a distance of 5 Å from the hetero atom of the crystal coordinate of COX-1 and COX-2 were removed retaining the catalytical water molecules at the active site receptor. Automatic, essential bonds, bond guidelines, crossbreeding, explicit-hydrogen, and charges were allocated. OPLS 2005 force field was applied to the protein to control minimization. RMSD of 0.30 Å was fixed to congregate heavy-weight particles through the pre-processing of protein former to docking. Accurate docking with flexible ligand sampling was adopted. Each ligand was docking into the receptor grid of radii 30 Å with x, y, z coordinates, and the docking calculation were adjudicated depending on the docking score with optimum ADMET values. A ligand-based ADMET calculation method was used to estimate the ADME/Tox properties of ligands.

Declarations

5. Acknowledgements

Fares Hezam Al-Ostoot is grateful to the public authority of Yemen and Al-Baydha University, Yemen, for giving monetary help under the instructor's association. Shaukath Ara Khanum, fortunately, recognizes the monetary help given by VGST, Bangalore, under CISEE Program [Project endorse request: No. VGST/CISEE/282]. Every one of the authors is grateful to the University of Mysore, Mysuru, India.

6. Declaration of interests

The authors confirm no contending monetary interest.

References

1. Khanum SA, Girish V, Suparshwa SS, Khanum NF (2009) Benzophenone-N-ethyl piperidine ether analogues-Synthesis and efficacy as anti-Inflammatory agent. Bioorg Med Chem Lett 19:1887–1891. https://doi.org/10.1016/j.bmcl.2009.02.070
2. Khanum SA, Venu TD, Shashikanth S, Firdouse A (2004) Synthesis and anti-inflammatory activity of newer analogues of dibenzoyl hydroxy phenyls. Bioorg Med Chem Lett 14:5351–5355. https://doi.org/10.1016/j.bmcl.2004.08.014
3. Khamees HA, Mohammed YH, Ananda S, Al-Ostoot FH, Sangappa Y, Alghamdi S, Khanum SA, Madegowda M (2020) Effect of o-difluoro and p-methyl substituents on the structure, optical properties and anti-inflammatory activity of phenoxy thiazole acetamide derivatives: Theoretical and experimental studies. J Mol Struct 1199:127024. https://doi.org/10.1016/j.molstruc.2019.127024
4. Zabiulla, Gulnaz AR, Mohammed YHE, A.Khanum S (2019) Design, synthesis and molecular docking of benzophenone conjugated with oxadiazole sulphur bridge pyrazole pharmacophores as anti-inflammatory and analgesic agents. Bioorg Chem 92:103220. https://doi.org/10.1016/j.bioorg.2019.103220
5. Kester M, Karpa KD, Vrana KE (2012) Pharmacokinetics. in: Elsevier's Integrated Review Pharmacology, Saunders, Elsevier
6. Kester M, Karpa KD, Vrana KE. Cancer and Immunopharmacology, in: Elsevier's Integrated Review Pharmacology, Elsevier. 2012:79–90. https://doi.org/10.1016/B978-0-323-07445-2.00005-7
7. Khanum SA, Shashikanth S, Deepak AV (2004) Synthesis and anti-inflammatory activity of benzophenone analogues. Bioorg Chem 32:211–212. https://doi.org/10.1016/j.bioorg.2004.04.003
8. Rawat C, Kukal S, Dahiya UR, Kukreti R (2019) Cyclooxygenase-2 (COX-2) inhibitors: future therapeutic strategies for epilepsy management. J Neuroinflammation 16:1–15. https://doi.org/10.1186/s12974-019-1592-3
9. Sauerschnig M, Stolberg-Stolberg J, Schmidt C, Wienerroither V, Plecko M, Schlichting K, Perka C, Dynybil C (2018) Effect of COX-2 inhibition on tendon-to-bone healing and PGE2 concentration after anterior cruciate ligament reconstruction. Eur J Med Res 23:1–11. https://doi.org/10.1186/s40001-017-0297-2
10. Al-Ostoot FH, Geetha DV, Mohammed YHE, Akhileshwari P, Sridhar MA, Khanum SA (2020) Design-based synthesis, molecular docking analysis of an anti-inflammatory drug, and geometrical optimization and interaction energy studies of an indole acetamide derivative. J Mol Struct 1202:127244. https://doi.org/10.1016/j.molstruc.2019.127244
11. Khamees HA, Mohammed YH, Swamynayaka A, Al-Ostoot FH, Sert Y, Alghamdi S, Khanum SA, Madegowda M (2019) Molecular structure, DFT, vibrational spectra with fluorescence effect, hirshfeld surface, docking simulation and antioxidant activity of thiazole derivative. ChemistrySelect 15:4544–4558.

https://doi.org/10.1002/slct.201900646

12. Rhodes S, Short S, Sharma S, Kaur R, Jha M (2019) One-pot mild and efficient synthesis of [1,3]thiazino[3,2-a]indol-4-ones and their anti-proliferative activity. Org Biomol Chem 17:3914–3920. https://doi.org/10.1039/C9OB00500E
13. Jismy B, Akssira M, Knez D, Guillaumet G, Gobec S, Abarbri M (2019) Efficient synthesis and preliminary biological evaluations of trifluoromethylated imidazo[1,2-a]pyrimidines and benzimidazo[1,2-a]pyrimidines. New J Chem 43:9961–9968. https://doi.org/10.1039/C9NJ01982K
14. Jampilek J (2019) Heterocycles in Medicinal Chemistry. Molecules 24:3839. https://doi.org/10.3390/molecules24213839
15. Hong F, Chen Y, Lu B, Cheng J (2016) One-Pot Assembly of Fused Heterocycles via Oxidative Palladium-Catalyzed Cyclization of Arylols and Iodoarenes. Adv Synth Catal 358:353–357. https://doi.org/10.1002/adsc.201500925
16. Lu F. Some Heterocyclic Polymers and Polysiloxanes, Macromol Sci J A. 1998;38:143–205. https://doi.org/10.1080/15583729808544527
17. Al-Ostoot FH, Stondus J, Anthal S, Venkatesh GD, Mohammed YHE, Sridhar MA, Khanum SA (2019) Kant. Synthesis, spectroscopic and X-ray crystallographic analysis of *N*-(2-(2-(4-chlorophenoxy) acetamido) phenyl)-1H-indole-2-carboxamide. Eur J Chem 10:234–238. https://doi.org/10.5155/eurjchem.10.3.234-238.1874
18. Caglar Yavuz S, Akkoc S, Turkmenoglu B, Sarıpınar E (2020) Synthesis of novel heterocyclic compounds containing pyrimidine nucleus using the Biginelli reaction: Antiproliferative activity and docking studies. J Heterocycl Chem 57:2615–2627. https://doi.org/10.1002/jhet.3978
19. Stamatiou G, Foscolos GB, Fytas G, Kolocouris A, Kolocouris N, Pannecouque C, Witvrouw M, Padalko E, Neyts J, De Clercq E (2003) Heterocyclic rimantadine analogues with antiviral activity. Bioorg Med Chem 11:5485–5492. https://doi.org/10.1016/j.bmc.2005.12.056
20. Kumar S, Singh RK, Patial B, Goyal S, Bhardwaj TR (2016) Recent advances in novel heterocyclic scaffolds for the treatment of drug-resistant malaria. J Enzyme Inhib Med Chem 31:173–186. https://doi.org/10.3109/14756366.2015.1016513
21. Desai NC, Pandya D, Vaja D (2018) Synthesis and antimicrobial activity of some heterocyclic compounds bearing benzimidazole and pyrazoline motifs. Med Chem Res 27:52–60. https://doi.org/10.1007/s00044-017-2040-5
22. Kumara K, Al-Ostoot FH, Mohammed YHE, Khanum SA, Lokanath NK (2019) Synthesis, crystal structure and 3D energy frameworks of ethyl 2-[5-nitro-2-oxopyridine-1 (2H)-yl] acetate: Hirshfeld surface analysis and DFT calculations. Chem Data Collect 20:100195. https://doi.org/10.1016/j.cdc.2019.100195
23. Altaf AA, Shahzad A, Gul Z, Rasool N, Badshah A, Lal B, Khan E (2015) A review on the medicinal importance of pyridine derivatives. J Drug Des Med Chem 1:1–11. https://doi.org/10.11648/j.jddmc.20150101.11
24. Al-Ostoot FH, Mohammed YHE, Zabiulla, Anup NK, Khanum SA. Synthesis, in silico study and in vitro anti-microbial evaluation of some new *N*-benzoyl-*N'*-[2-(4-chloro-phenoxy)-acetyl]-hydrazides analogs. J Appl Pharm Sci 2019;9:042–049. https://doi.org/10.7324/JAPS.2019.90706
25. Mohan M, Satyanarayan MN, Trivedi DR (2019) Exploring the possibilities of double proton transfer in hydrazides; A theoretical approach. J Phys Org Chem 32:4003. https://doi.org/10.1002/poc.4003
26. Shen S, Chen H, Zhu T, Ma X, Xu J, Zhu W, Chen R, Xie J, Ma T, Jia L, Wang Y, Peng C (2017) Synthesis, characterization and anticancer activities of transition metal complexes with a nicotinohydrazone ligand. Oncol Lett 13:3169–3176. https://doi.org/10.3892/ol.2017.5857
27. Khanum SA, Khanum NF, Shashikanth M (2008) Synthesis and anti-inflammatory activity of 2-aryloxy methyl oxazolines, Bioorg. Med Chem Lett 18:4597–4601. https://doi.org/10.1016/j.bmcl.2008.07.029
28. Brooks P, Kubler P (2006) Etoricoxib for arthritis and pain management. Ther Clin Risk Manag 2:45–57. PMID: 18360581
29. Salehi B, Sestito S, Rapposelli S, Peron G, Calina D, Sharifi-Rad M, Sharopov F, Martins N. Epibatidine (2016) A Promising Natural Alkaloid in Health Biomolecules 9:6. https://doi.org/10.3390/biom9010006
30. Tilve GH, Lengade JK, Bavadekar AV, Nair KG (1976) Niflumic acid in the management of rheumatoid and osteoarthritis. J Postgrad Med 22:124–129. https://www.jpgmonline.com/text.asp?1976/22/3/124/42844
31. Boyce S, Webb JK, Shepheard SL, Russell MGN, Hill RG, Rupniak NMJ (2000) Analgesic and toxic effects of ABT-594 resemble epibatidine and nicotine in rats. Pain 85:443–450. https://doi.org/10.1016/S0304-3959(99)00303-6
32. Dudek K, Bednarek D, Ayling RD, Kycko A, Reichert M (2019) Preliminary study on the effects of enrofloxacin, flunixin meglumine and pegbovigrastim on Mycoplasma bovis pneumonia. BMC Vet Res 15:1–13. https://doi.org/10.1186/s12917-019-2122-3
33. Bertram GK. Basic and Clinical Pharmacology: McGraw-Hill Companies. New York. 2001;8:596- 7
34. Collier HOJ, Dinneen LC, Johnson CA, Schneider C (1968) The abdominal constriction response and its suppression by analgesic drugs in the mouse. Br J Pharmacol 32:295–310. https://doi.org/10.1111/j.1476-5381.1968.tb00973.x
35. Williamson EM, Okpako DT, Evans FJ. Selection (1996) Preparation and Pharmacological Evaluation of Plant Material, 1. John Wiley & Sons, Chichester, pp 184–186
36. Thapa R, Sai K, Saha D, Kushwaha D, Aswal VK, Moulick RG, Bose S, Bhattaharya J (2021) Synthesis and characterization of a nanoemulsion system for solubility enhancement of poorly water soluble non-steroidal anti-inflammatory drugs. J Mol Liq 334:115998. https://doi.org/10.1016/j.molliq.2021.115998
37. Rowlinson SW, Kiefer JR, Prusakiewicz JJ, Pawlitz JL, Kozak KR, Kalgutkar AS, Stallings WC, Kurumbail RG, Marnett LJ (2003) J Biol Chem 278:45763–45769. https://doi.org/10.1074/jbc.M305481200
38. Praveen Rao PN, Amini M, Li H, Habeeb AG, Knaus EE (2003) Design, Synthesis, and Biological Evaluation of 6-Substituted-3-(4-methanesulfonylphenyl)-4-phenylpyran-2-ones: A Novel Class of Diarylheterocyclic Selective Cyclooxygenase-2 Inhibitors. J MedChem 46:4872–4882. https://doi.org/10.1021/jm0302391

39. Zou H, Yuan C, Dong L, Sidhu RS, Hong YH, Kuklev DV (2012) Human cyclooxygenase-1 activity and its responses to COX inhibitors are allosterically regulated by nonsubstrate fatty acids. J Lipid Res 53:1336–1347. https://doi.org/10.1194/jlr.M026856
40. Swarup A, Agarwal R, Malhotra S, Dube AS (2016) A comparative study of efficacy of gabapentin in inflammation induced neuropathic animal pain models with conventional analgesic diclofenac. Int J Res Med Sci 4:1429–1432. http://dx.doi.org/10.18203/2320-6012.ijrms20161204
41. Koster R, Anderson M, De Beer EJ. Acetic Acid for Analgesic Screening. InFed proc. 1959;18:412-7. https://ci.nii.ac.jp/naid/10029461846/
42. Arrigoni-Martelli E (1979) Screening and assessment of anti-inflammatory drugs. Find Exp Clin Pharmacol 1:157–177. https://ci.nii.ac.jp/naid/20000739254/
43. Fakhr IM, Radwan MA, El-Batran S, Abd El-Salam OM, El-Shenawy SM (2009) Synthesis and pharmacological evaluation of 2-substituted benzo [b] thiophenes as anti-inflammatory and analgesic agents. Eur J Med Chem 44:1718–1725. https://doi.org/10.1016/j.ejmech.2008.02.034
44. Natesh R, Schwager SLU, Sturrock ED, Acharya KR (2003) Crystal structure of the human angiotensin-converting enzyme–lisinopril complex. Nature 421:551–554. https://doi.org/10.1038/nature01370
45. Williams LK, Zhang X, Caner S, Tysoe C, Nguyen NT, Wicki J, Williams DE, Coleman J, McNeill JH, Yuen V, Andersen RJ, Withers SG, Brayer GD (2015) The amylase inhibitor montbretin A reveals a new glycosidase inhibition motif. Nat Chem Biol 11:691–696. https://doi.org/10.1038/nchembio.1865

Tables

Table 1: COX-1 and COX-2 enzyme *in-vitro* inhibition of compounds (**9a-e** and **10a-e)**.

Compound	IC50 (μM)[a]		COX-2SI[b]
	COX-1	COX-2	
9a	8.156	0.213	38.29
9b	10.537	0.159	66.27
9c	9.756	0.118	82.67
9d	6.907	0.207	33.36
9e	10.011	0.101	99.11
10a	9.016	0.165	54.64
10b	10.088	0.133	75.84
10c	10.895	0.11	99.04
10d	8.590	0.263	32.66
10e	11.107	0.095	116.91
Celecoxib	14.820	0.091	162.85
Diclofenac	4.802	0.822	5.84
Indomethacin	0.041	0.502	0.08

[a]In vitro concentration of synthesized compound that produce 50% inhibition of COX-1and COX-2 enzymes, the result (IC_{50}, μM) is the mean of two values obtained using an ovine COX-1/COX-2 assay. The deviation from the mean is<10% of the mean value.[b]Thein vitro COX-2 selectivity index (COX-1 IC_{50}/COX-2 IC_{50}).

Table 2: Anti-inflammatory activity of compounds (**9a-e** and **10a-e).**

Compounds	Paw volume change (ml)				% Edema inhibition				IC50μM
	1h	2h	3h	6h	1h	2h	3h	6h	
9a	1.4 ±0.02*	1.6±0.10	1.8±0.33	2.6±0.25	34.55	30.40	25.95	10.01	11.98±0.29
9b	1.2±0.08*	1.1±0.01	1.3±0.14	2.2±0.13	42.88	43.60	45.92	22.65	09.87±0.55
9c	1.2 ± 0.08*	1.1 ± 0.4*	1.0 ± 0.14*	1.8 ± 0.22*	46.99	55.71	60.89	39.99	6.99±0.10
9d	1.6 ± 0.26	1.9 ± 0.02	2.1 ± 0.17	2.6 ± 0.40	25.75	20.51	14.98	10.02	12.65±0.42
9e	1.3 ± 0.10*	1.3 ± 0.02*	1.3 ± 0.06*	1.5 ± 0.35*	38.83	40.34	45.78	45. 85	7.9±0.41
10a	1.1 ± 0.17*	1.3 ± 0.20*	1.5 ± 0.24*	2.0 ± 0.05*	46.95	45. 33	37. 93	30.02	8.4±0.20
10b	1.0 ± 0.05*	1.0 ± 0.11*	1.0 ± 0.11*	1.5 ± 0.17*	51.76	55.75	60.91	45.82	7.68±0.12
10c	1.2 ± 0.04*	1.1 ± 0.12*	1.1 ± 0.12*	1.7 ± 0.21*	42.99	47. 52	56.95	39.90	6.91±0.30
10d	1.90 ± 0.13	1.8 ± 0.03	1.7 ± 0.11	1.9 ± 0.16*	12.93	19.45	29.98	32.88	8.98±0.21
10e	1.0 ± 0.06*	0.9 ± 0.33*	0.8 ± 0.12*	1.5 ± 0.33*	51.99	57. 21	64. 92	45. 95	7.75±0.39
Vehicle	2.3 ± 0.27	2.4 ± 0.06	2.5 ± 0.08	3.0 ± 0.34	0	0	0	0	-
Diclofenac	1.5 ± 0.17*	1.7 ± 0.4	1.9 ± 0.31	2.2 ± 0.42	30.32	25.42	22.86	22.88	9.7±0.41

Values are means ± SEM (n=3-4) significantly different from the normal control group at p < 0.05.*

Table 3: Analgesic effect of compounds (**9a-e** and **10a-e)** on acetic acid induced writhing response

Compounds	Number of writhing	% inhibition	IC50μM
9a	34.66±1.98	27.65	11±0.29
9b	19.68±2.33	57.55	7.9±0.52
9c	28.93±0.75*	38.88	10.2±0.2
9d	36.35±1.19	24.76	11.9±0.39
9e	28.80±0.75*	38.89	10.5±0.43
10a	21.82±2.53	53.94	8.9±0.28
10b	24.96±1.97	47.66	8.3±0.12
10c	17.44±2.12	62.67	5.9±0.29
10d	36.84±2.02	23.34	10.7±0.19
10e	16.99±2.74*	63.48	5.9±0.39
Vehicle	48.93± 4.91	0	-
Piroxicam	16.86±2.32*	63.99	7.1±0.38

*Data represent the mean value ± SE of four mice per group. Drugs were, s.c., administered 30 min before testing. Statistical comparisons are made between control group and synthesized compounds treated group and denoted by p < 0.05 * significantly different from the normal control group at p < 0.05.*

Table 4: Analgesic effect of compounds (**9a-e** and **10a-e)** on thermal pain induced by a hot plate method

Compounds	Basal	1 h		2 h		IC50μM
		Latency time (s)*	% Latency change	Latency time (s)*	% Latency Change	
9a	18 ± 2.8	26 ± 3.7*	41.73	25 ± 3.9*	35.99	11±0.34
9b	14 ± 3.6	21± 3.6	45.90	21 ± 6.3	45.94	9.2±0.34
9c	17 ± 3.5	26 ± 1.9*	49.97	24 ± 3.3*	37.94	8.9±0.02
9d	17 ± 6.4	22 ± 2.9	26.95	21 ± 4.8	21.89	12.2±0.37
9e	17 ± 6.2	26 ± 1.1*	49.77	18 ± 1.9*	45.75	8.5±0.37
10a	18 ± 2.0	26 ± 1.0*	41.90	18 ± 1.9*	45.93	8.9±0.48
10b	18 ± 2.9	27 ± 2.0*	46. 32	25 ± 3.2*	35.99	7.8±0.10
10c	13 ± 3.4	25 ± 1.4*	84.91	26 ± 2.3*	49.29	8.6±0.29
10d	14 ± 4.1	16 ± 1.9	12.83	15 ± 1.52	05.96	19.8±0.21
10e	12 ± 3.1	23 ± 1.1*	89.95	21 ± 6.1*	56.64	6.9±0.29
Saline	17 ± 4.6	16 ± 5.2	0	14 ± 1.0	0	-
Piroxicam	14 ± 4.7	26 ± 2.0*	76.70	25 ± 2.1*	72.87	6.2±0.37

Note: *Values are means ± SD of four mice per group. Statistical comparisons between basal and post-drug values were analyzed for statistical significance using one-way ANOVA test and denoted by $p < 0.05$.* significantly different from the normal control group at $p < 0.05$*

Table 5: Docking scores of synthesized compounds **9(a-e)** and **10(a-e)** against COX-1 and COX-2.

Protein	COX1 (PDB ID: 3KK6)					COX2 (PDB ID: 4COX)				
Compound	**Docking Score**	**Glide evdw**	**Glide Energy**	**Glide emodel**	**XP HBond**	**Docking Score**	**Glide evdw**	**Glide Energy**	**Glide emodel**	**XP HBond**
10a	-7.74	-42.22	-43.70	-62.05	0.00	-5.43	-31.54	-36.45	-55.20	-0.22
10b	-8.54	-42.67	-43.52	-61.41	0.00	-8.94	-38.26	-41.91	-60.76	0.00
10c	-7.77	-32.93	-33.17	-52.59	0.00	-8.96	-40.55	-44.71	-55.10	0.00
10d	-6.72	-35.52	-36.05	-53.65	0.00	-8.31	-37.85	-41.79	-60.04	-0.11
10e	**-8.41**	**-40.75**	**-41.17**	**-57.55**	**-0.11**	**-8.98**	**-36.37**	**-40.55**	**-53.91**	**-0.35**
9a	-7.64	-34.48	-35.42	-57.72	0.00	-7.73	-25.32	-32.19	-50.14	-0.35
9b	-8.35	-41.12	-42.97	-53.46	-0.23	-8.45	-33.98	-37.34	-50.95	-0.11
9c	-7.87	-33.33	-36.41	-44.44	0.00	-8.32	-40.25	-42.03	-58.46	0.00
9d	-6.99	-32.79	-35.71	-52.37	-0.20	-6.77	-33.79	-38.04	-58.79	-0.22
9e	-8.38	-40.94	-42.63	-54.58	-0.30	-7.25	-35.18	-37.54	-54.92	-0.63
Celecoxib	-12.65	-36.57	-47.33	-68.28	0.00	-10.58	-43.74	-47.45	-63.22	-0.90
Diclofenac	-8.06	-35.32	-35.12	-48.68	0.00	-8.57	-26.19	-28.81	-40.97	-0.31
Indomethacin	-10.83	-43.96	-44.61	-62.47	0.00	-12.18	-38.88	-45.40	-66.09	-1.73

Table 6: ADME/Tox evaluation of compounds **9(a-e)** and **10(a-e)**.

Compound	a*	b*	c*	d*	e*	f*	g*	h*	i*	j*	k*	l*	m*	n*	o*	p*
9a	30.57	10.26	14.62	9.84	2.04	-3.38	-3.15	-6.16	422.56	194.97	-1.16	-2.40	4.0	-0.26	85.89	0.0
9b	31.85	10.85	15.31	9.59	2.53	-4.11	-3.84	-6.07	423.94	482.29	-1.01	-2.57	4.0	-0.15	88.77	0.0
9c	33.17	11.41	15.96	9.36	3.02	-4.73	-4.54	-5.94	469.89	1194.56	-0.82	-2.62	4.0	-0.04	92.45	0.0
9d	32.41	10.45	15.13	9.53	2.35	-3.94	-3.43	-6.07	424.07	195.73	-1.20	-2.60	5.0	-0.11	87.70	0.0
9e	32.22	10.98	15.45	9.60	2.61	-4.23	-4.74	-6.10	424.11	518.78	-1.01	-2.57	4.0	-0.13	89.23	0.0
10a	30.58	10.26	14.62	9.84	2.04	-3.39	-3.15	-6.16	422.48	194.93	-1.16	-2.40	4.0	-0.26	85.89	0.0
10b	31.86	10.85	15.28	9.60	2.53	-4.12	-3.84	-6.09	431.62	491.73	-1.01	-2.55	4.0	-0.15	88.94	0.0
10c	33.23	11.43	15.95	9.38	3.03	-4.76	-4.54	-5.98	473.03	1204.10	-0.83	-2.60	4.0	-0.04	92.56	0.0
10d	32.41	10.45	15.13	9.53	2.35	-3.94	-3.43	-6.07	423.69	195.54	-1.20	-2.60	5.0	-0.11	87.69	0.0
10e	32.21	10.97	15.42	9.61	2.61	-4.24	-4.74	-6.13	431.27	528.22	-1.00	-2.55	4.0	-0.13	89.39	0.0
Indomethacin	35.53	11.18	17.27	9.77	4.27	-5.10	-5.09	-3.23	167.30	224.48	-0.65	-2.64	3.0	0.04	91.73	0.0
Diclofenac	28.00	9.87	13.83	7.88	4.50	-5.31	-4.80	-3.02	377.77	783.30	-0.18	-1.78	4.0	0.03	100.00	0.0
Celecoxib	38.17	10.74	19.77	11.94	3.33	-5.80	-5.73	-5.71	354.74	786.28	-0.77	-3.24	1.0	0.37	92.08	0.0
Standard Range	13.0 to 70.0	4.0 to 18.0	8.0 to 35.0	4.0 to 45.0	-2.0 to 6.5	-6.5 to 0.5		< -5	<25 poor, >500 great		-3.0 to 1.2	–	1.0 to 8.0	-1.5 to 1.5	<25% is poor	Max is 4

Note:a:QPpolrz;b*:QPlogPC16;c*:QPlogPoct;d*:QPlogPw;e*:QPlogPo/w;f*:QPlogS; g*:ClQPlogS;h*:QPlogHERG;i*:QPPCaco;j*:QPPMDCK; k*:QPlogBB;l*:QPlogKp; m*:No. of metabolites; n*:QPlogKhsa; o*:Percent human oral absorption;p*:Rule of five.*

Figures

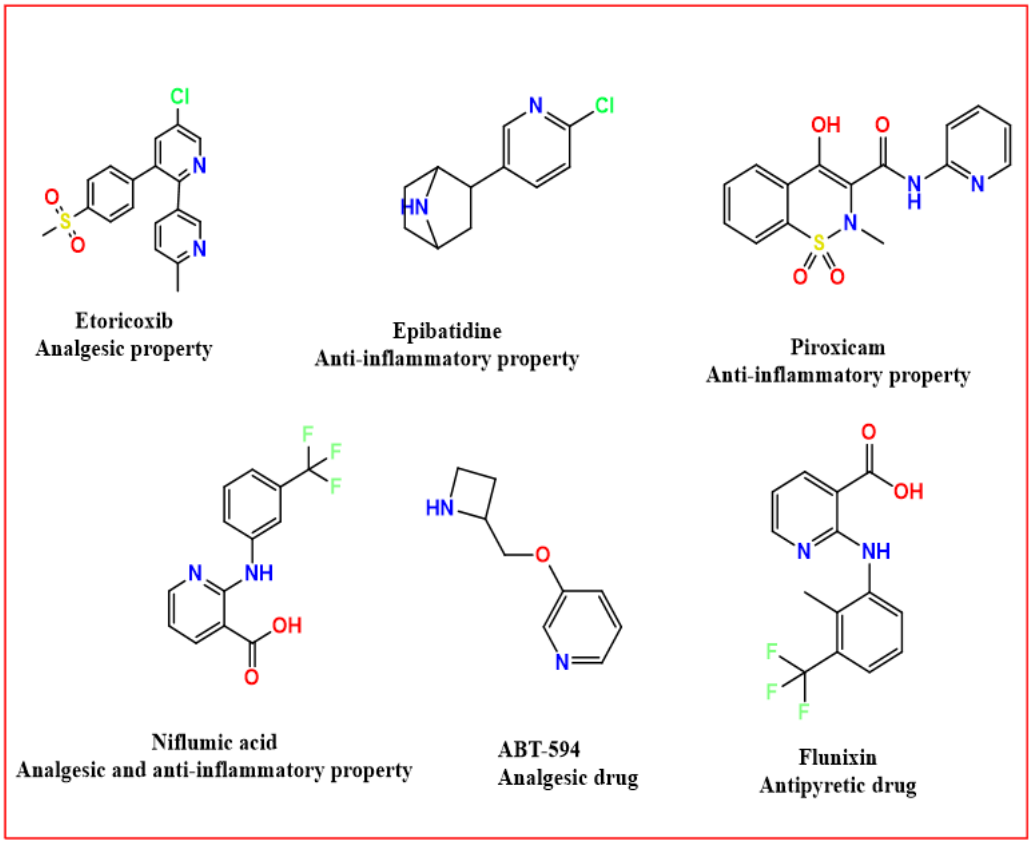

Figure 1

Pyridine core containing drugs with their biological activities.

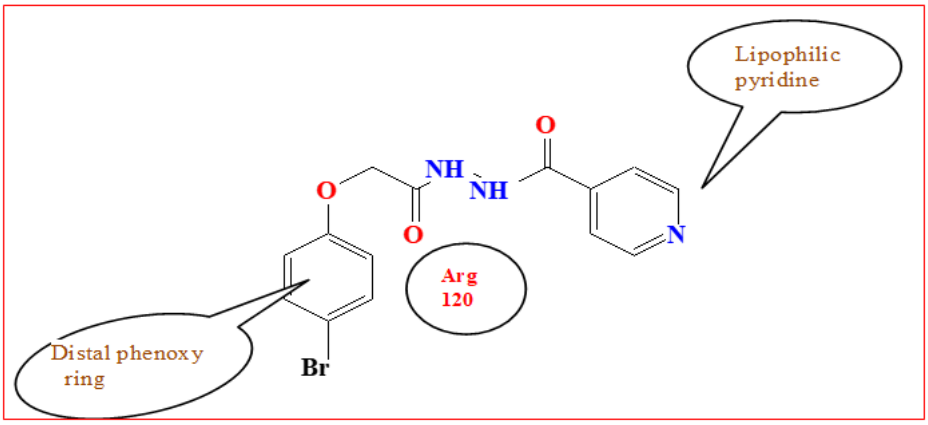

Figure 2

Design strategy of compound (10e).

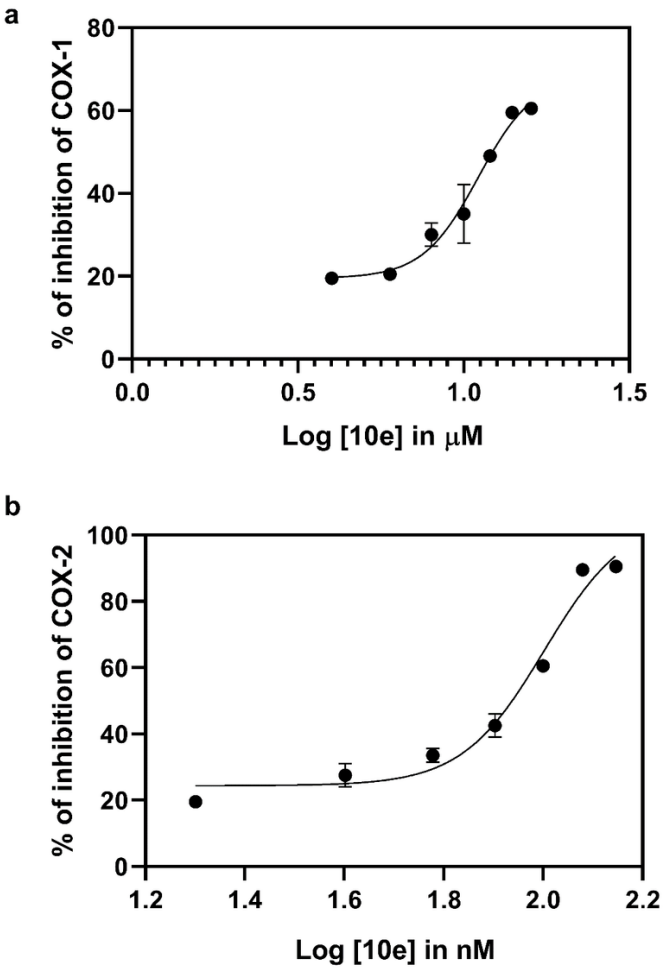

Figure 3

Normalized dose response curves showing the effect of (10e) on COX-1 (a) and COX-2 (b). IC50 was calculated using sigmoidal four-parameter logistic curve (4PL) plot. All data values represent mean ± SEM (n = 5).

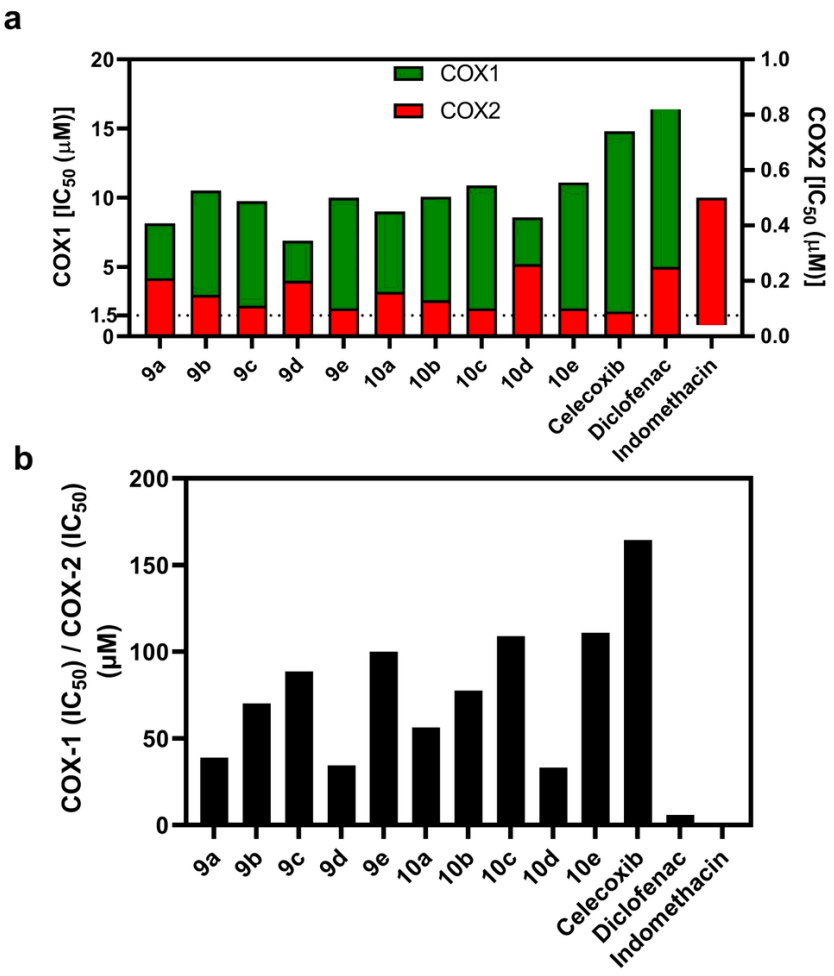

Figure 4

Graphical representation of IC50 (COX-1 and COX-2) values for the 9(a-e) and 10(a-e) in comparison with celecoxib, diclofenac and indomethacin (a). Comparative analysis to differentiate selective and non-selective COX-2 inhibitory activity for 9(a-e) and 10(a-e), with an imaginary trend line (b). All data values represent mean ± SEM (n = 5).

Figure 5

Effect of compound 10e on carrageenan-induced paw edema in mice. Typical representative macroscopic photographs of paw from the Normal (a), Carrageenan + Saline (b), Carrageenan + Indomethacin (c), Carrageenan + compound 10e (d). Treated.

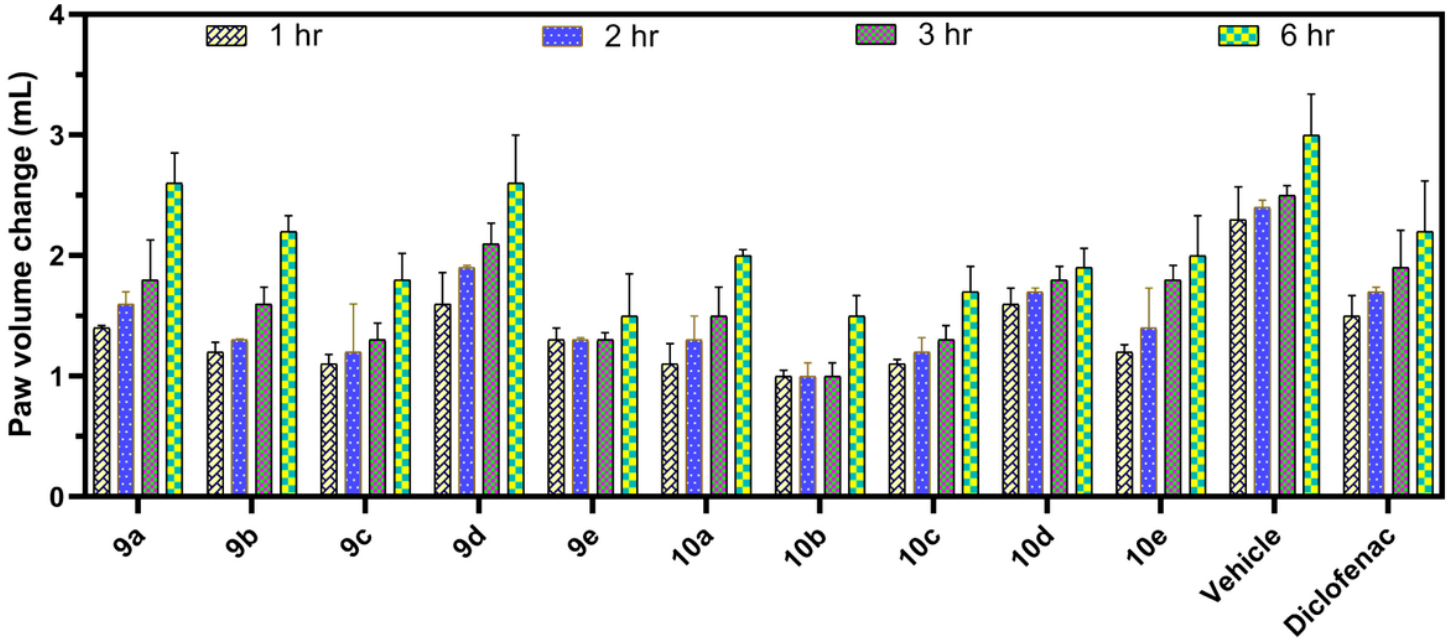

Figure 6

Neutralization of edema-inducing activity of formalin by 9(a-e) and 10(a-e). All data values represent mean±SEM (n=4).

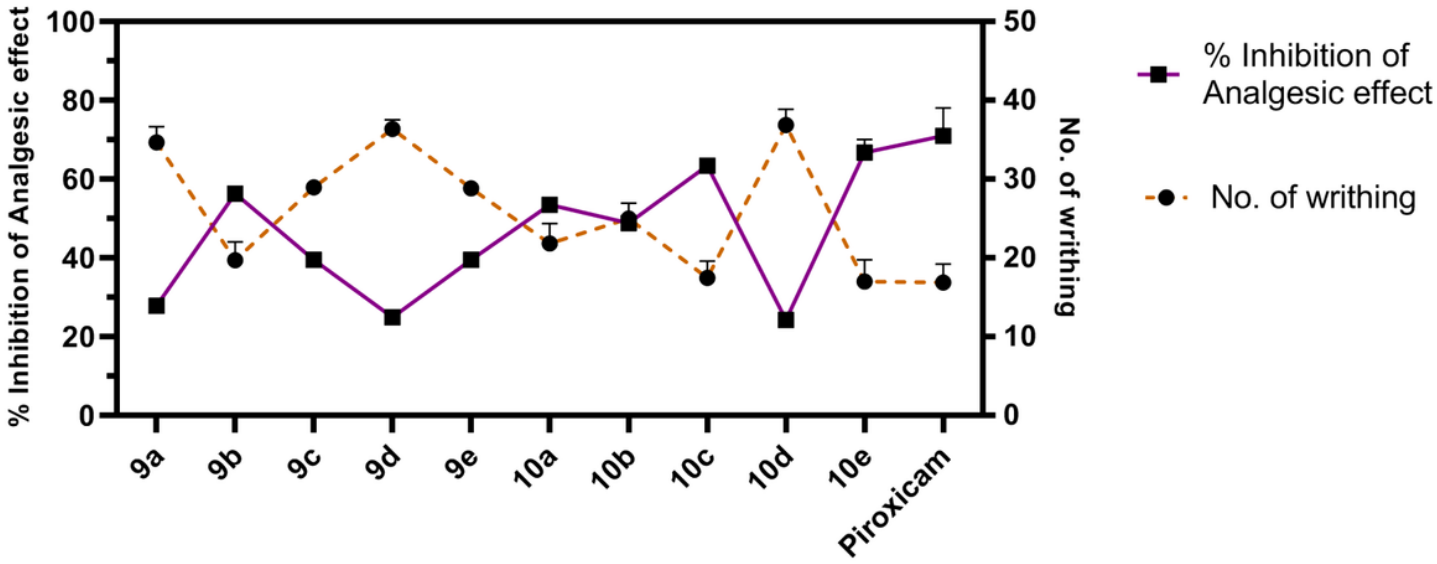

Figure 7

Analgesic effect of compounds 9(a-e) and 10(a-e) on acetic acid induced writhing response.

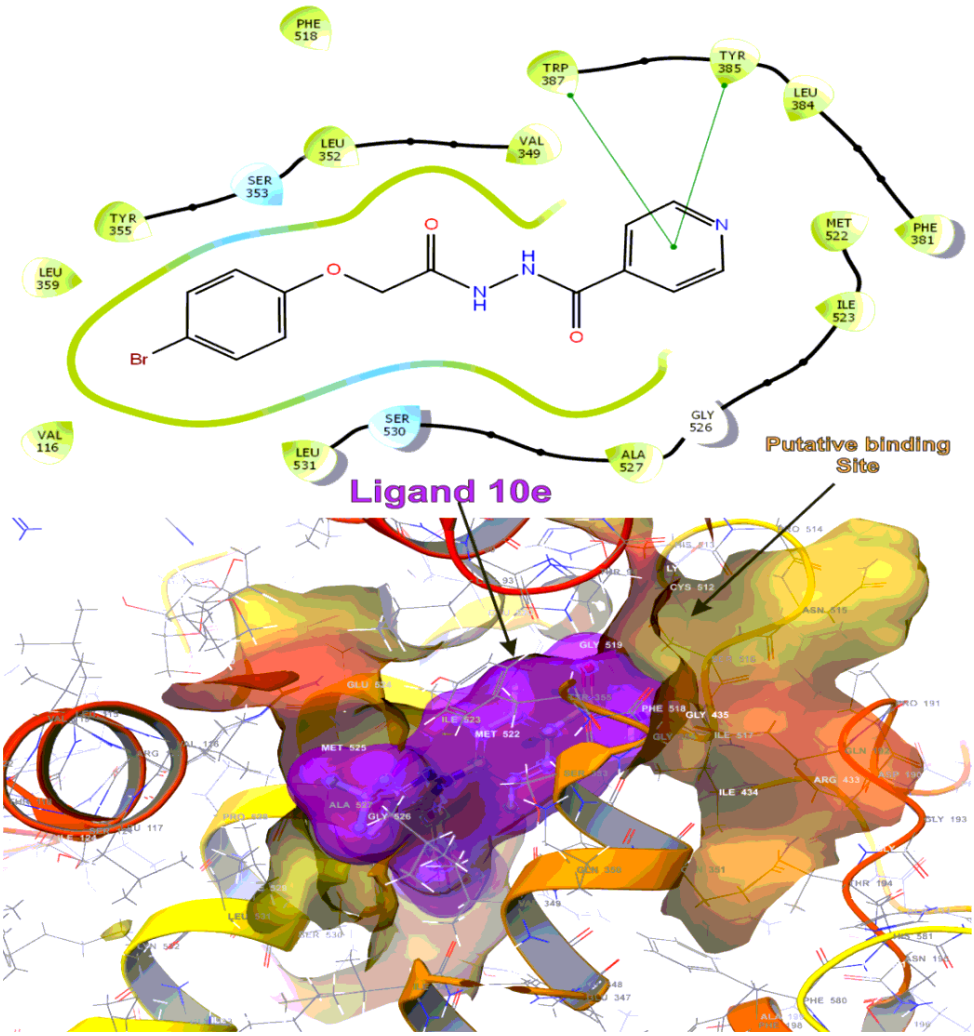

Figure 8

The lowest energy conformation of docking result of ligand (10e) with COX-1 (3KK6). The three dimensional putative binding cavity of COX-1 is represented in olive yellow mixed with light orange and the ligand in dark pink.

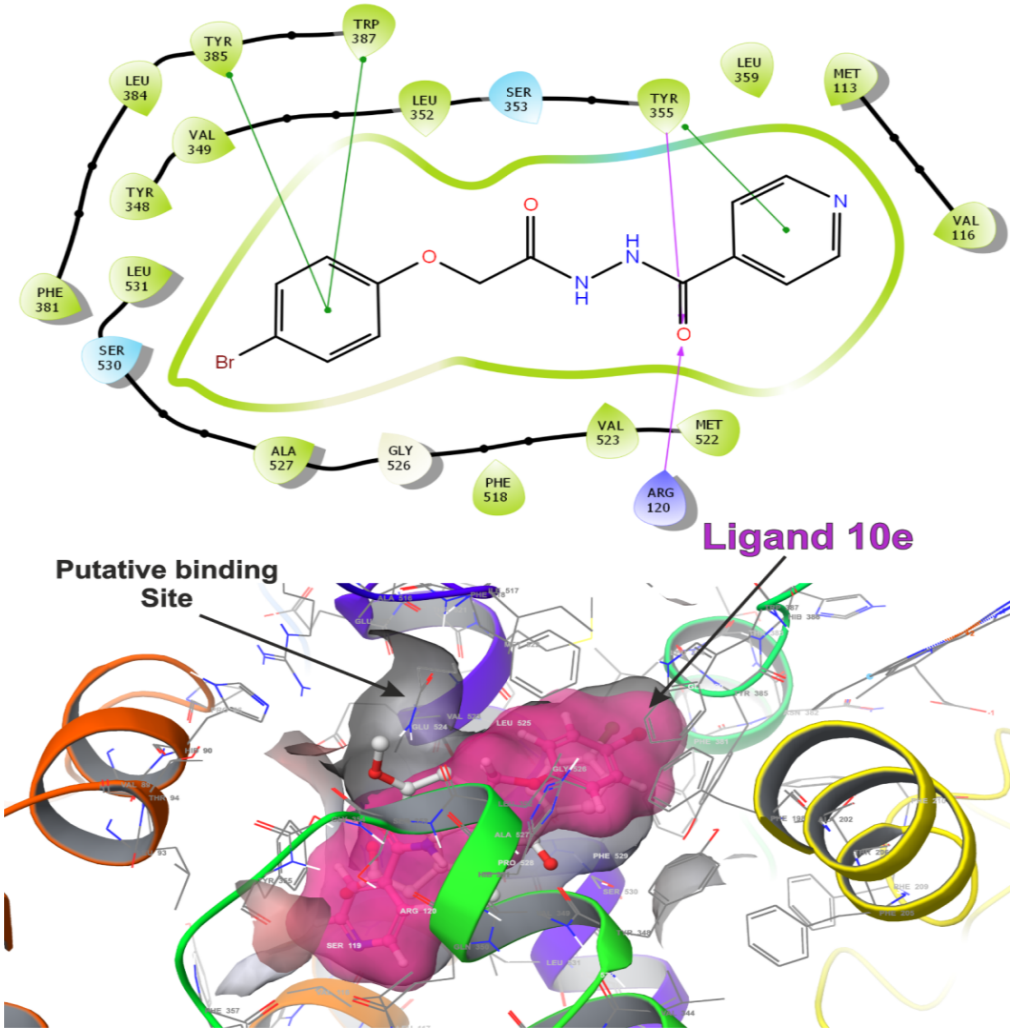

Figure 9

The lowest energy conformation of docking result of ligand (10e) with COX-2 (4COX). The three dimensional putative binding cavity of COX-2 is represented in solid grey and the ligand in dark pink.

Supplementary Files

This is a list of supplementary files associated with this preprint. Click to download.

- Scheme1.png
- Graphicalabstract.docx
- supplementaryfile.docx